THE JOURNAL OF PHYSICAL CHEMISTRY Letters

Letter

pubs.acs.org/JPCL

Polymeric Frameworks as Organic Semiconductors with Controlled Electronic Properties

Ken Sakaushi,*[,†,§,#] Georg Nickerl,[§] Hem Chandra Kandpal,[‡,§] Laura Cano-Cortés,[‡] Thomas Gemming,[†] Jürgen Eckert,[†,¶] Stefan Kaskel,[§] and Jeroen van den Brink*[,‡]

[†]Institute for Complex Materials and [‡]Institute for Theoretical Solid State Physics, IFW Dresden, Helmholtzstrasse 20, D-01069 Dresden, Germany

[§]Department of Inorganic Chemistry, TU Dresden, Bergstrasse 66, D-01069 Dresden, Germany

[§]Department of Chemistry, Indian Institute of Technology Roorkee, Roorkee-247 667, India

[¶]Institute of Materials Science, TU Dresden, Helmholtzstrasse 7, D-01069 Dresden, Germany

Supporting Information

ABSTRACT: The rational assembly of monomers, in principle, enables the design of a specific periodicity of polymeric frameworks, leading to a tailored set of electronic structure properties in these solid-state materials. The further development of these emerging systems requires a combination of both experimental and theoretical studies. Here, we investigated the electronic structures of two-dimensional polymeric frameworks based on triazine and benzene rings by means of electrochemical techniques. The experimental density of states was obtained from quasi-open-circuit voltage measurements through a galvanostatic intermittent titration technique, which we show to be in excellent agreement with first-principles calculations performed for two- and three-dimensional structures of these polymeric frameworks. These findings suggest that the electronic properties depend not only on the number of stacked layers but also on the ratio of the different aromatic rings.

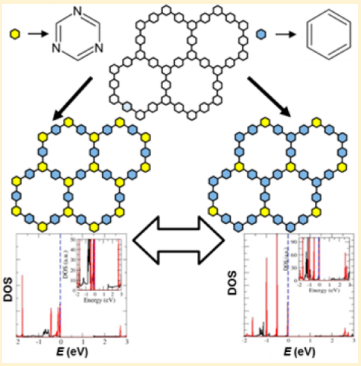

SECTION: Energy Conversion and Storage; Energy and Charge Transport

Since the discovery of conductive polymers,[1−3] semiconducting conjugated polymers have been of great interest in organic electronics applications,[4,5] such as organic electroluminescent diodes,[6−9] photovoltaic cells,[10,11] photocatalyst polymers,[12] and organic batteries.[13−16] One of the most interesting properties pursued by organic electronics is bipolarity, existence of both p- and n-type semiconducting behavior in the same material.[17] This feature is not only important from a fundamental scientific viewpoint but also for its possible applications; bipolar organic compounds are promising candidates to promote further development of the field of organic electronics.[18] The discovery of bipolarity in a new class of organic materials can foster future developments of the above-mentioned technologies.[19] Indeed, recent works on π-conjugated microporous polymers show that polymeric frameworks are promising materials for organic electronics[20,21] and even for organic spintronics.[22] The experimental control of structural periodicities by choosing a monomer as the building block of the framework can lead to semiconducting systems with unique electronic properties, such as two-dimensional (2D) atomic crystals.[23] The possibility of controlling bipolar organic semiconductors' electronic properties can give rise to new electronic system-level design[24] based on artificial semiconducting polymeric frameworks, which would represent a giant leap forward in the development of organic electronic devices.

Here, we studied the electronic properties of covalent triazine-based frameworks[25] (CTFs) by performing electrochemical measurements and comparing with first-principles electronic structure calculations. The CTFs are porous polymeric frameworks formed by cyclotrimerization of nitrile monomers, which have been applied in the implementation of catalyst materials[26,27] and most recently for lithium- and sodium-based energy storage devices.[28,29] They have a conjugated structure, consisting of benzene rings as electron donors and triazine rings as electron acceptors (Figure 1), with controllable photoluminescent properties.[30] Despite the above-mentioned properties, surprisingly, little work has been done in the study of CTFs toward an efficient implementation in organic electronics. In a previous study, we have carried out several electrochemical measurements to test the electrochemical properties of electrode materials, such as CTFs.[28,29] From these experiments, important information about the electronic structure of materials[31−33] can be obtained. Thus, we applied these electrochemical techniques in the present work to investigate the tunability of the electronic properties of porous polymeric frameworks, testing their properties as organic

Received: June 26, 2013
Accepted: August 20, 2013
Published: August 20, 2013

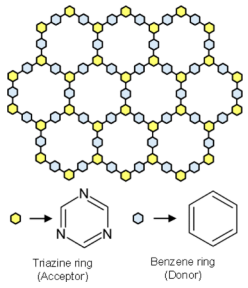

Figure 1. Schematic illustration for the ideal CTF composed of benzene and triazine rings with a ratio of 1:1.5, so-called CTF-1.

semiconductors, which we combined with a theoretical study of the density of states (DOS) for two CTFs compounds.

We synthesized a CTF porous polymeric framework consisting of triazine and benzene rings in the theoretical ratio of 1:1.5, so-called CTF-1. By performing a careful tuning of the synthetic conditions, we can obtain the crystalline form of CTF-1, which has a 2D structure with an eclipsed AAA stacking and *P6/mmm* symmetry. We characterized CTF-1 by using spectroscopic measurements. In this sense, Raman spectroscopy measurements (RSMs) can reveal the electronic structure of materials, as well as information about the associated structural periodicity. Because the structures of the analogous organic systems graphite and graphene have been extensively studied by RSMs,[34−38] we compared the Raman spectra of CTF-1 and graphite (Figure 2a). In this case, the multilayer and monolayer CTF-1 is comparable to N-doped porous graphite and N-doped porous graphene, respectively. The *G* peak is produced by the doubly degenerated zone center E_{2g} mode, which corresponds to the motion of the atoms in the 2D honeycomb structure.[34−36] The *D* peak, which is an inactive mode for perfect graphite, is induced by disorder in the 2D structure.[34,36] The peak at ∼2700 cm^{-1} is historically called the *G′* peak, but using the same notation as that in refs 36 and 38, we call this peak 2*D*. The comparison of the *D*-to-*G* intensity ratio,[37] $I(D)/I(G)$, for CTF-1 (1.1) and graphite (0.3), suggests that CTF-1 has a shorter 2D ordered structure (Figure 2a). However, the existence of the *G* peak for CTF-1 clearly reveals the formation of a 2D honeycomb structure composed of benzene and triazine rings. Electron energy-loss spectroscopy (EELS) measurements were carried out to have further information about the structure of CTF-1 (Figure 2b). The fine features of C-*K* and N-*K* edges indicate sp^2-bonding, characteristic of graphitic networks.[39] The 1s → π^* transition observed confirms the sp^2-hybridization for carbon and nitrogen atoms at ∼285 (Figure 2b) and ∼400 eV (Figure 2b inset), respectively. Therefore, by performing Raman and EELS experiments, we confirmed the formation of a 2D polymeric framework composed of aromatic rings. In addition, high-resolution transmission electron microscopy (HR-TEM) observation (Figure 2c) showed the stacking of 2D sheets of CTF-1 with ∼10 layers (Figure 2c inset). The porous structure of CTF-1 cannot be clearly observed due to multiple sheets stacking and the resolution of HR-TEM imaging. However, N_2 physisorption experiments (Figure 2d) indicate the existence of a porous structure of the CTF-1 with a pore diameter of ∼14 Å, which is in good agreement with the pore size of the perfect crystalline CTF-1 (Figure 2d). These results reveal the formation of CTF-1 with 2D ordering. Therefore, covalent triazine polymeric frameworks show controllable electronic properties and semiconducting character due to a graphene-like structural periodicity, combined with a suitable choice of the monomer as a building block.

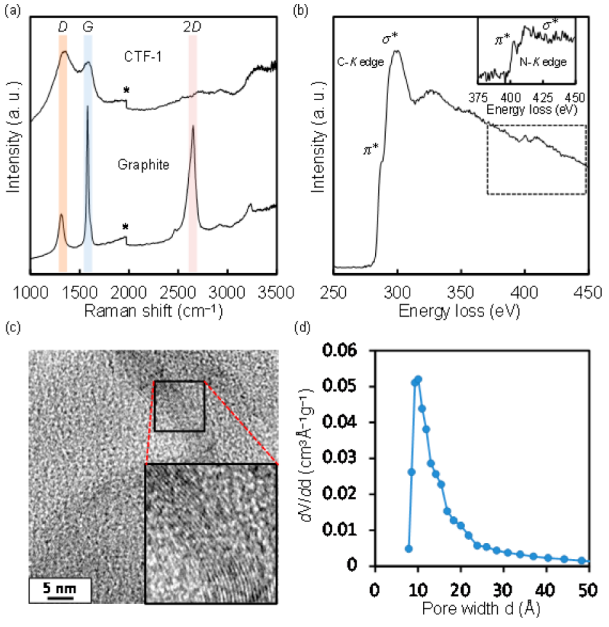

Figure 2. (a) Raman spectrum for CTF-1 and graphite; ∗ indicates the artificial step due to the equipment. (b) EEL spectrum for CTF-1. The inset shows the N-*K* edge (the dotted area) with the extraction of background. (c) HR-TEM image of CTF-1. The inset shows the edge of CTF-1, showing a stacking of layers. (d) Pore width distribution of CTF-1.

We measured open-circuit voltage (OCV) (=E_{OCV}) curves through the galvanostatic intermittent titration technique (GITT) to investigate the quasi-equilibrium states[40,41] of CTF-1 (Figure 3a,b). The bipolarity observed in this material is derived from the electron-donor and electron-acceptor character of the benzene and triazine rings, respectively.[25,28] Thus, CTF-1 can have both an n-doped state (negatively charged state; Figure 3c) and a p-doped state (positively charged state; Figure 3d). It has been suggested in previous

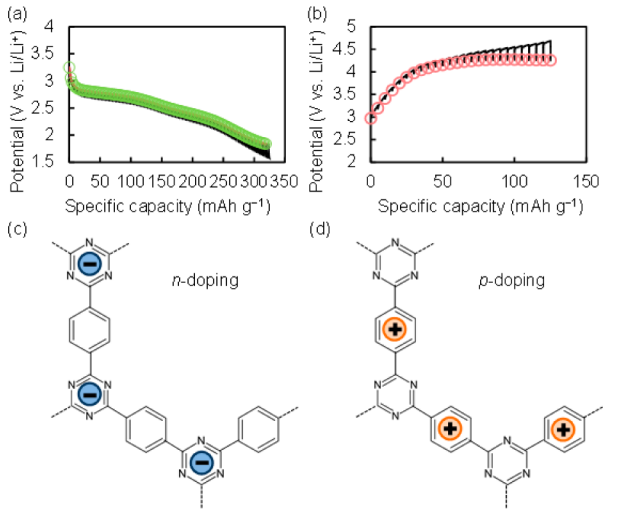

Figure 3. (a) OCV curve at n-doping. (b) OCV curve at p-doping. (c) Schematic illustration of n-doping at triazine rings (acceptor). (d) Schematic illustration of p-doping at benzene rings (donor).

dx.doi.org/10.1021/jz401316x | *J. Phys. Chem. Lett.* 2013, 4, 2977−2981

electrochemical measurements on the porous polymeric frameworks as electrodes with $LiPF_6$ in ethylene carbonate/dimethyl carbonate (1:1) as the electrolyte that Li^+ and PF_6^- are coordinated with CTFs based on a redox mechanism.[28] Electrochemical properties of polymeric frameworks as electrodes are directly connected with their electronic structures.[42,43] For the n-doping process (Li^+ reaction), we found a plateau at ~2.7 V versus Li/Li^+ and the following sloping curve in a discharge curve (Figure 3a). The slope of this OCV curve is different from the ones obtained for typical intercalation compounds, which show a plateau followed by a sharp drop in the potential.[32] In the p-doping process (PF_6^- reaction), we observed a plateau at ~4.2 V versus Li/Li^+ (Figure 3b). Although the details of the energy storage mechanism of porous polymeric frameworks are still unclear, previous works on the adatom of both cations and anions into graphite,[44−46] graphene,[45−49] and related materials suggest that the ions could be coordinated on the top of the aromatic rings, which serve as hosts. This unique electrochemical reaction should correspond to the electronic structure of CTF-1.

On the basis of the above discussion, we described the relation between the OCV measurements and the electronic structure of CTF-1 by means of thermodynamics and statistical mechanics.[31−33,50] The potential given by OCV depends on the chemical potential, $\mu(x)$, of the guest (Li), where x is the amount of inserted guest in a host material, and it is described by the Nernst equation, as follows:

$$E_{OCV}(x) = \frac{-\mu(x)}{e} \tag{1}$$

We consider the lattice-gas model, in which each site of the lattice has two states, full or empty. Then, we can define the occupancy of the guest sites, $f(\varepsilon)$, as a function of energy, ε, through the Fermi distribution at the voltage E_{OCV}

$$f(\varepsilon) = \frac{n(\varepsilon)}{N(\varepsilon)} = \frac{1}{1 + \exp\left(\frac{\varepsilon - \mu}{k_B T}\right)} \tag{2}$$

where $N(\varepsilon)$ is the number of sites with energy ε and $n(\varepsilon)$ is the number of occupying Li ions. From eqs 1 and 2, we derive the relation between $n(\varepsilon)$ and E_{OCV}

$$n(\varepsilon) = \frac{N(\varepsilon)}{1 + \exp\left(\frac{\varepsilon + eE_{OCV}}{k_B T}\right)} \tag{3}$$

Equation 4 shows the integration of $n(\varepsilon)$ over the entire energy range, giving us the number of intercalated Li ions in the polymeric framework, n

$$n = \int_{-\infty}^{+\infty} \frac{g(\varepsilon)}{1 + \exp\left(\frac{\varepsilon + eE_{OCV}}{k_B T}\right)} d\varepsilon \tag{4}$$

Here, we have defined the distribution of the site energy as $g(\varepsilon) = dN(\varepsilon)/d\varepsilon$.

For ideal bulk electrodes, one finds a flat plateau in the OCV potential curves due to the fact that all sites have a specific energy, ε_i, thus equating $g(\varepsilon)$ to a delta function $\delta(\varepsilon - \varepsilon_i)$ in eq 4. In the case of anisotropic and/or disordered electrode materials, the value for the occupation energy is broadened, $\Delta\varepsilon$. This energy distribution for the sites of the guest is reflected in the change in the slope of OCV curves, where the steepness that is observed for ideal electrodes is reduced, resulting in smoother slopes. Thus, if we assume a monolayer or completely disordered CTF-1, following eq 4, we would expect a smooth slope OCV curve without any plateau. This can be understood from the modification of the electronic structure of CTF-1 due to both anisotropy and the existence of defects.[31−33] However, CTF-1 shows a plateau, which confirms that this polymeric framework is partially formed by an ordered multilayer structure (Figure 2c).

The distribution of the site energy can be obtained from the charge and discharge curves in the OCV measurements, giving us the DOS, $g(\varepsilon)$. From the GITT technique, we obtain the DOS from the relation dQ/dE_{OCV}, where the capacity Q (mA h/g) is the total quantity of electrons involved in the electrochemical reaction per unit cell and dE_{OCV} (V) is determined by the number of sites with energy ε. We calculated the experimental DOS (Figure 4a) by analyzing the OCV

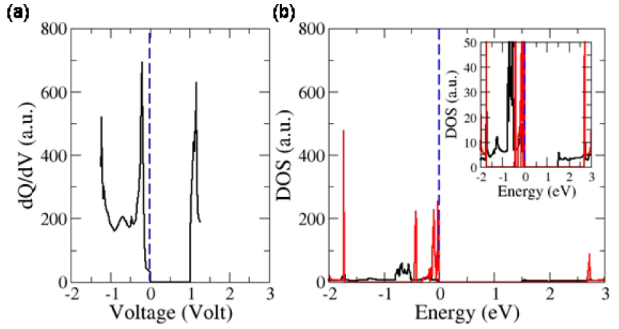

Figure 4. (a) Measurement of the DOS as a function of the voltage for the CTF-1. (b) Theoretical DOS for the ideal CTF-1 for the single layer (red) and the bulk case (black), obtained from ab initio calculations. The inset presents the same data in a more illustrative fashion. The voltage (a) and energy (b) are given with respect to the Fermi level (dashed blue line).

curves (Figure 3a,b) for the CTF-1, which is formed by multilayer sheets (up to ~10 layers) of 2D polymeric frameworks (Figure 2c). Then, we studied CTF-1 through first-principles calculations on a monolayer and a multilayer system using the all-electron full-potential local orbital (FPLO) code,[51,52] version 9.01-35 within the generalized gradient approximation (GGA).[53] The valence basis set consists of carbon (1s, 2s, 2p, 3s, 3p, 3d), nitrogen (1s, 2s, 2p, 3s, 3p, 3d), and hydrogen (1s, 2s, 2p) states. All atoms including hydrogen atoms were relaxed using a force evaluated in a scalar relativistic mode with a convergence criterion of 1 meV/Å. The monolayer is modeled with 20 Å spacing along the z-direction, which is large enough to avoid the interaction between the two consecutive interlayers. Self-consistent calculations employed a grid of 6912 (multilayer) and 2500 (monolayer) k points in the full Brillouin zone. From the calculations, we extract the theoretical DOS (Figure 4b) for the 2D (red) and 3D (black) case. Due to the quasi-two-dimensional character of the CTF-1 multilayered system, a direct comparison of the experimental band gap, ~1.4 eV, with the monolayer, ~2.7 eV, and the multilayer gap, ~1.5 eV, is not relevant. A main feature in both DOSs is a large peak close to the Fermi level, which is indicative of the existence of flat bands and charge localization.

One of the most important aspects in the study of CTFs is the ratio of the aromatic rings used in the synthesis process and how the electrochemical properties are affected by this. We synthesized a polymeric framework in which triazine and

dx.doi.org/10.1021/jz401316x | J. Phys. Chem. Lett. 2013, 4, 2977−2981

benzene rings have the ratio of 1:4 (here, we call it CTF-TCPB; see Supporting Information Figure S1 and S2 for the experimental results of CTF-TCPB). We also calculated the DOS and compared the results with the case of CTF-1. From Figure S2a in the Supporting Information and Figure 4b, we observed several peaks in the DOS right below the Fermi level for CTF-1, while in the case of CTF-TCPB, the peaks are shifted to lower energies. This indicates a more conducting behavior for CTF-1 when doping the system (holes) than for that of CTF-TCPB. Indeed, the cyclic voltammetry (CV) measurements for CTF-1 and CTF-TCPB confirmed this result (Supporting Information Figure S2b). While CTF-1 exhibited a continuous CV due to the larger peak density in the DOS, CTF-TCPB clearly showed two separated redox reactions due to its different electronic structure. From the latest comparison, we conclude that we can tune the electronic structure properties of CTFs by changing the periodicity of either the frameworks or the aromatic rings in these systems.

In summary, we studied the electronic structure of CTFs by combining electrochemical experimental techniques and theoretical studies. Our results reveal that the particular electronic structure of CTFs emerges from their structural periodicity and that their electronic properties are controllable by changing the number of layers and the ratio of benzene and triazine aromatic rings. Therefore, covalent triazine polymeric frameworks can lead to further development of organic semiconductors with tunable electronic properties, where band gaps and doping properties can be controlled by combining the donor/acceptor character of the starting monomers in the synthesis of these frameworks.

EXPERIMENTAL SECTION

Synthesis of Porous Polymeric Frameworks. The CTFs were synthesized by ionothermal synthesis as described in ref 25, heating a mixture of *p*-dicyanobenzene or tris(4-cyanophenyl benzene) and $ZnCl_2$ in quartz ampules at 400 °C for 40 h. The obtained samples were washed with 1 M HCl and distilled water several times. The nitrogen physisorption measurements were carried out at 77 K up to 1 bar using a Quantachrome Autosorb 1C apparatus. The pore size distribution was obtained by applying the QS-DFT equilibrium model for nitrogen on carbon with slit pores at 77 K.

Physical Characterization for Porous Polymeric Frameworks. The electron energy-loss spectrum (EELS) measurement was carried out using a Tecnai F30 (FEI company) operated at an accelerating voltage of 300 kV by using a special sample holder that can keep the organic specimen cool. The RSMs were carried out by using a NIR Raman spectrometer HoloLab Series 5000 from Kaiser Optical Systems with a laser excitation of 785 nm and a power of 10 mW on the sample.

Electrochemistry. The polymeric frameworks were characterized by their electrochemical properties. The electrodes were made by the polymeric framework (70 wt %), conductive additive (Super-P; 20 wt %), and binder (carboxyl methyl cellulose; 10 wt %). We used Al foils as a current collector. We assembled the two-electrode Swagelok-type cells in an argon-filled glovebox and tested them on a multichannel potentiostatic-galvanostatic system (VMP-3, Bio-Logic). We used lithium metal as an anode and 1 M $LiPF_6$ in ethylene carbonate and dimethyl carbonate (volume ratio 1:1) as an electrolyte.

Theoretical Study. We performed electronic structure calculations in the framework of density functional theory (DFT) using the full potential local-orbital scheme implemented in FPLO codes.[51,52] The exchange−correlation energy functional was evaluated within the GGA using the Perdew, Burke, and Ernzerhof parametrization.[53] We used previous reported data[25] on the crystal structure of CTF-1 and calculated the DOS corresponding to the ground-state energy of the optimized geometry of the system for monolayers and bulk multilayers of CTF-1 and CTF-TCPB compounds. The geometry optimization was carried out by evaluating the atomic forces on each atom with a convergence criterion of 1 meV/Å.

ASSOCIATED CONTENT

Supporting Information

Additional figures, including Raman spectra, HR-TEM images, and the theoretical DOS for CTF-TCPB and cyclic voltammograms of CTF-1 and CTF-TCPB. This material is available free of charge via the Internet at http://pubs.acs.org.

AUTHOR INFORMATION

Corresponding Authors

*E-mail: ken.sakaushi@mpikg.mpg.de (K.S.).
*E-mail: j.van.den.brink@ifw-dresden.de (J.v.d.B.).

Present Address

#K.S.: Max Planck Institute for Colloids and Interfaces, Research Campus Potsdam-Golm, D-14424 Potsdam, Germany.

Notes

The authors declare no competing financial interest.

ACKNOWLEDGMENTS

K.S. would like to thank Dr. Susanne Machill (TU Dresden) for Raman spectroscopy measurements. K.S. is supported by the German Academic Exchange Service, DAAD (Grant No.: A/09/74990).

REFERENCES

(1) Akamatsu, H.; Inokuchi, H.; Matsunaga, Y. Electronic Conductivity of the Perylene−Bromine Complex. *Nature* **1954**, *173*, 168.
(2) Shirakawa, H.; Louis, E. J.; MacDiarmid, A. G.; Chiang, C. K.; Heeger, A. J. Synthesis of Electrically Conducting Organic Polymers: Halogen Derivatives of Polyacetylene, $(CH)_x$. *J. Chem. Soc., Chem. Commun.* **1977**, 578−580.
(3) Chiang, C. K.; Fincher, C. R.; Park, Y. W.; Heeger, A. J.; Shirakawa, H.; Louis, E. J.; Gau, S. C.; MacDiarmid, A. G. Electrical Conductivity in Doped Polyacetylene. *Phy. Rev. Lett.* **1977**, *39*, 1098−1101.
(4) Forrest, S. R.; Thomson, M. E. Introduction: Organic Electronics and Optoelectronics. *Chem. Rev.* **2007**, *107*, 923−925.
(5) Walzer, K.; Maennig, B.; Pfeiffer, M.; Leo, K. Highly Efficient Organic Devices Based on Electrically Doped Transport Layers. *Chem. Rev.* **2007**, *107*, 1233−1271.
(6) Tang, C. W.; VanSlyke, S. A. Organic Electroluminescent Diodes. *Appl. Phys. Lett.* **1987**, *51*, 913−915.
(7) Burroughes, J. H.; Bradley, D. D. C.; Brown, A. R.; Marks, R. N.; Mackay, K.; Friend, R. H.; Burns, P. L.; Holmes, A. B. Light-Emitting Diodes Based on Conjugated Polymers. *Nature* **1990**, *347*, 539−541.
(8) Kido, J.; Kimura, M.; Nagai, K. Multilayer White Light-Emitting Organic Electroluminescent Device. *Science* **1995**, *267*, 1332−1334.
(9) Friend, R. H.; Gymer, R. W.; Holmes, A. B.; Burroughes, J. H.; Marks, R. N.; Taliani, C.; Bradley, D. D. C.; Dos Santos, D. A.; Brédas, J. L.; Lögdlund, M.; Salaneck, W. R. Electroluminescent in Conjugated Polymers. *Natrue* **1999**, *397*, 121−128.
(10) Tang, C. W. Two-Layer Organic Photovoltaic Cell. *Appl. Phys. Lett.* **1986**, *48*, 183−185.

(11) Brabec, C. J.; Sariciftci, N. S.; Hummelen, J. C. Plastic Solar Cells. *Adv. Funct. Mater.* **2001**, *11*, 15−26.
(12) Wang, X. C.; Maeda, M.; Thomas, A.; Takanabe, K.; Xin, G.; Carlsson, J. M.; Domen, K.; Antonietti, M. A Metal-Free Polymeric Photocatalyst for Hydrogen Production from Water under Visible Light. *Nat. Mater.* **2009**, *8*, 76−80.
(13) Nigrey, P. J.; MacInnes, D.; Nairns, D. P.; MacDiarmid, A. G.; Heeger, A. J. Lightweight Rechargeable Storage Batteries Using Polyacetylene, $(CH)_x$ as the Cathode-Active Material. *J. Electrochem. Soc.* **1981**, *128*, 1651−1654.
(14) Novák, P.; Müller, K.; Santhanam, K. S. V.; Haas, O. Electrochemically Active Polymers for Rechargeable Batteries. *Chem. Rev.* **1997**, *97*, 207−281.
(15) Liang, Y.; Tao, Z.; Chen, J. Organic Electrode Materials for Rechargeable Lithium Batteries. *Adv. Energy Mater.* **2012**, *2*, 742−769.
(16) Hayashi, K.; Matsuishi, S.; Kamiya, T.; Hirano, M.; Hosono, H. Light-Induced Conversion of an Insulating Refractory Oxide into a Persistent Electronic Conductor. *Nature* **2002**, *419*, 462−465.
(17) Yanagi, H.; Ueda, K.; Ohta, H.; Orita, M.; Hirano, M.; Hosono, H. Fabrication of All Oxide Transparent *p*−*n* Homojunction Using Bipolar $CuInO_2$ Semiconducting Oxide with Delafossite Structure. *Solid State Commun.* **2001**, *121*, 15−17.
(18) Zaumseil, J.; Sirringhaus, H. Electron and Ambipolar Transport in Organic Field-Effect Transistors. *Chem. Rev.* **2007**, *107*, 1296−1323.
(19) Feng, X.; Chen, L.; Honsho, H.; Saengsawang, O.; Liu, L.; Wang, L.; Saeki, A.; Irle, S.; Seki, S.; Dong, Y.; Jiang, D. An Ambipolar Conducting Covalent Organic Framework with Self-Sorted and Periodic Electron Donor−Acceptor Ordering. *Adv. Mater.* **2012**, *24*, 3026−3031.
(20) Cooper, A. I. Conjugated Microporous Polymers. *Adv. Mater.* **2009**, *21*, 1291−1295.
(21) Weber, J.; Bojdys, M. J; Thomas, A. Polymeric Frameworks: Toward Porous Semiconductors. In *Supramolecular Soft Matter: Applications in Materials and Organic Electronics*Nakanishi, T., Ed.; John Wiley & Sons, Inc.: Hoboken, NJ, 2011.
(22) Du, A.; Sanvito, S.; Smith, S. C. First-Principle Prediction of Metal-Free Magnetism and Intrinsic Half-Metallicity in Graphitic Carbon Nitride. *Phys. Rev. Lett.* **2012**, *108*, 197207.
(23) Novoselov, K. S.; Jiang, D.; Schedin, F.; Booth, T. J.; Khotkevich, V. V.; Morozov, S. V.; Geim, A. K. Two-Dimensional Atomic Crystals. *Proc. Natl. Acad. Sci. U.S.A.* **2005**, *102*, 10451−10453.
(24) Yang, P. D.; Tarascon, J. M. Towards Systems Materials Engineering. *Nat. Mater.* **2012**, *11*, 560−563.
(25) Kuhn, P.; Thomas, A.; Antonietti, M. Porous, Covalent Triazine-Based Frameworks Prepared by Ionothermal Synthesis. *Angew. Chem., Int. Ed.* **2008**, *47*, 3450−3453.
(26) Palkovits, R.; Antonietti, M.; Kuhn, P.; Thomas, A.; Schüth, F. Solid Catalysts for the Selective Low-Temperature Oxidation of Methane to Methanol. *Angew. Chem., Int. Ed.* **2009**, *48*, 6909−6912.
(27) Schwinghammer, K.; Tuffy, B.; Mesch, M. B.; Wirnhier, E.; Martineau, C.; Taulelle, F.; Schnick, W.; Senker, J.; Lotsch, B. V. Triazine-Based Carbon Nitrides for Visible-Light-Driven Hydrogen Evolution. *Angew. Chem., Int. Ed.* **2013**, *52*, 2435−2439.
(28) Sakaushi, K.; Nickerl, G.; Wisser, F. M.; Nishio-Hamane, D.; Hosono, E.; Zhou, H. S.; Kaskel, S.; Eckert, J. An Energy Storage Principle Using Bipolar Porous Polymeric Frameworks. *Angew. Chem., Int. Ed.* **2012**, *51*, 7850−7854.
(29) Sakaushi, K.; Hosono, E.; Nickerl, G.; Gemming, T.; Zhou, H. S.; Kaskel, S.; Eckert, J. Aromatic Porous-Honeycomb Electrodes for a Sodium-Organic Energy Storage Device. *Nat. Commun.* **2013**, *4*, 1485.
(30) Ren, S.; Bojdys, M. J.; Dawson, R.; Laybourn, A.; Khimyak, Y. Z.; Adams, D. J.; Cooper, A. I. Porous, Fluorescent, Covalent Triazine-Based Frameworks via Room-Temperature and Microwave-Assisted Synthesis. *Adv. Mater.* **2012**, *24*, 2357−2361.
(31) Kudo, T.; Hibino, M. Consideration on the Potential-Composition Relationships Observed with Amorphous Intercalation Systems such as Li_xWO_3. *Solid State Ionics* **1996**, *84*, 65−72.
(32) Okubo, M.; Hosono, E.; Kim, J.; Enomoto, M.; Kojima, N.; Kudo, T.; Zhou, H. S.; Honma, I. Nanosized Effect on High-Rate Li-Ion Intercalation in $LiCoO_2$ Electrode. *J. Am. Chem. Soc.* **2007**, *129*, 7444−7452.
(33) Okubo, M.; Kim, J.; Kudo, T.; Zhou, H. S.; Honma, I. Anisotropic Surface Effect on Electronic Structures and Electrochemical Properties of $LiCoO_2$. *J. Phys. Chem. C* **2009**, *113*, 15337−15342.
(34) Tuinstra, F.; Koenig, J. L. Raman Spectrum of Graphite. *J. Chem. Phys.* **1970**, *53*, 1126−1130.
(35) Lespade, P.; Al-Jishi, R.; Dresselhaus, M. S. Model for Raman Scattering from Incompletely Graphitized Carbons. *Carbon* **1982**, *20*, 427−431.
(36) Reich, S.; Thomsen, C. Raman Spectroscopy of Graphite. *Philos. Trans. R. Soc. London, Ser. A* **2004**, *362*, 2271−2288.
(37) Ferrari, A. C.; Robertson, J. Raman Spectroscopy of Amorphous, Nanostructured, Diamond-Like Carbon, and Nanodiamond. *Philos. Trans. R. Soc. London, Ser. A* **2004**, *362*, 2477−2512.
(38) Ferrari, A. C.; Meyer, J. C.; Scardaci, V.; Casiraghi, C.; Lazzeri, M.; Mauri, F.; Piscanec, S.; Jiang, D.; Novoselov, K. S.; Roth, S.; Geim, A. K. Raman Spectrum of Graphene and Graphene Layers. *Phys. Rev. Lett.* **2006**, *97*, 187401.
(39) Thomas, A.; Fischer, A.; Goettmann, F.; Antonietti, M.; Müller, J.-O.; Schlögl, R.; Carlsson, J. M. Graphitic Carbon Nitride Materials: Variation of Structure and Morphology and Their Use as Metal-Free Catalysts. *J. Mater. Chem.* **2008**, *18*, 4893−4908.
(40) Weppner, W.; Huggins, R. A. Determination of the Kinetics Parameters of Mixed Conducting Electrodes and Application to the System Li_3Sb. *J. Electrochem. Soc.* **1977**, *124*, 1569−1578.
(41) Yamada, A.; Koizumi, H.; Nishimura, S.-H.; Sonoyama, N.; Kanno, R.; Yonemura, M.; Nanamura, T.; Kobayashi, Y. Room-Temperature Miscibility Gap in Li_xFePO4. *Nat. Mater.* **2006**, *5*, 357−360.
(42) Pahdi, A. K.; Nanjundaswamy, K. S.; Masquelir, C.; Okada, S.; Goodenough, J. B. Effect of Structure on the Fe^{3+}/Fe^{2+} Redox Couple in Iron Phosphates. *J. Electrochem. Soc.* **1997**, *144*, 1609−1613.
(43) Goodenough, J. B.; Kim, Y. Challenges for Rechargeable Li Batteries. *Chem. Mater.* **2010**, *22*, 587−603.
(44) Dzurus, M. L.; Henning, G. R. Properties of the Interstitial Compounds of Graphite. IV. Properties of N-Type Compounds. *J. Chem. Phys.* **1957**, *27*, 275−281.
(45) Dahn, J. R.; Zheng, T.; Liu, Y.; Xue, J. S. Mechanism for Lithium Insertion in Carbonaceous Materials. *Science* **1995**, *270*, 590−593.
(46) Winter, M.; Besenhard, J. O.; Spahr, M. E.; Novák, P. Insertion Electrode Materials for Rechargeable Lithium batteries. *Adv. Mater.* **1998**, *10*, 725−763.
(47) Wang, S.; Matsumura, Y.; Maeda, T. A Model of the Interactions Between Disordered Carbon and Lithium. *Synth. Met.* **1995**, *71*, 1759−1760.
(48) Zheng, T.; Xing, W.; Dahn, J. R. Carbons Prepared from Coals for Anodes of Lithium-Ion Batteries. *Carbon* **1996**, *34*, 1501−1507.
(49) Profeta, G.; Calandra, M.; Mauri, F. Phonon-Mediated Superconductivity in Graphene by Lithium Deposition. *Nat. Phys.* **2012**, *8*, 131−134.
(50) Morikazu, T.; Kubo, R.; Saito, N. *Statistical Physics I: Equilibrium Statistical Mechanics*; Springer: New York, 1992.
(51) Koepernik, K.; Eschrig, H. Full-Potential Nonorthogonal Local-Orbital Minimum-Basis Band-Structure Scheme. *Phy. Rev. B* **1999**, *59*, 1743−1757.
(52) FPLO Homepage. http://www.fplo.de (2013).
(53) Perdew, J. P.; Burke, K.; Ernzerhof, M. Generalized Gradient Approximation Made Simple. *Phys. Rev. Lett.* **1996**, *77*, 3865−3868.